Commun. Comput. Phys.
doi: 10.4208/cicp.290610.060411a

Vol. **11**, No. 3, pp. 726-738
March 2012

A Spectral Iterative Method for the Computation of Effective Properties of Elastically Inhomogeneous Polycrystals

Saswata Bhattacharyya*, Tae Wook Heo, Kunok Chang and Long-Qing Chen

Department of Materials Science and Engineering, The Pennsylvania State University, University Park, PA 16802, USA.

Received 29 June 2010; Accepted (in revised version) 6 April 2011

Available online 28 October 2011

Abstract. We report an efficient phase field formalism to compute the stress distribution in polycrystalline materials with arbitrary elastic inhomogeneity and anisotropy. The dependence of elastic stiffness tensor on grain orientation is taken into account, and the elastic equilibrium equation is solved using a spectral iterative perturbation method. We discuss its applications to computing residual stress distribution in systems containing arbitrarily shaped cavities and cracks (with zero elastic modulus) and to determining the effective elastic properties of polycrystals and multilayered composites.

AMS subject classifications: 74B10, 74S25

Key words: Elasticity, spectral method, iterative method.

1 Introduction

Phase-field models have been extensively used to study the effect of elastic stresses on microstructural evolution during solid-to-solid phase transformations (see the reviews [1–3] for details). However, most of these models approximate the elastic modulus to be homogeneous. Homogeneous modulus approximation is not a valid assumption when the microstructures exhibit large elastic inhomogeneity. Examples of elastically inhomogeneous materials include multiphase materials in which the constituent phases have different elastic moduli, composites, systems containing cavities and cracks, and polycrystalline materials. In the case of polycrystals, the overall elastic stiffness tensor depends

*Corresponding author. *Email addresses:* sxb57@psu.edu (S. Bhattacharyya), tuh134@psu.edu (T. W. Heo), kuc142@psu.edu (K. Chang), lqc3@psu.edu (L.-Q. Chen)

on the orientation of each grain constituting the polycrystal. As a result, polycrystalline materials are always associated with an inhomogeneous distribution of elastic moduli.

There have been fewer efforts to model elastically inhomogeneous systems using phase field models. Leo et al. and Zhu et al. numerically solved the mechanical equilibrium equation for elastically inhomogeneous systems using conjugate gradient method [4, 5]. Hu and Chen developed an iterative-perturbation scheme to solve the mechanical equilibrium equation in elastically inhomogeneous binary alloys [6, 7]. Wang et al. developed a phase field microelasticity theory to model elastically and structurally inhomogeneous solids [8]. Their theory is based on the estimation of strain energy of an elastically inhomogeneous solid by numerically computing the effective stress free strain for an equivalent elastically homogeneous system [8, 9].

In this paper we present a phase field model based on the iterative-perturbation method developed by Hu and Chen [6] to compute the residual stress distribution in polycrystalline materials. This allows one to compute the equilibrium stress distribution for any arbitrary structurally and elastically inhomogeneous microstructure using our method. Furthermore, it will be shown that the effective elastic properties of polycrystals can be efficiently computed from its response to an applied stress or strain.

2 Formulation and numerical implementation

In the phase-field model developed by Fan and Chen for studying grain growth [10, 11], a polycrystalline microstructure is described using a set of Q continuous, non-conserved order parameter fields $\eta_i(\mathbf{r},t)$ $(i=1,\cdots,Q)$. The order parameter fields represent grains of a given crystallographic orientation. We use a function $\phi(\mathbf{r},t)=\sum_i \eta_i^2(\mathbf{r},t)$ to distinguish between the grain interior and the grain boundaries.

In a polycrystalline material, the elastic constants depend on the relative orientation of different grains constituting the polycrystal and hence are always inhomogeneous. Since the grains are rotated with respect to a fixed coordinate system, the elastic stiffness tensor for each grain is obtained by transforming the tensor with respect to the fixed coordinate system. Let C_{ijkl} represent the stiffness tensor for a single grain in a fixed reference frame. Then, the position-dependent elastic stiffness tensor for the entire polycrystal in terms of the order parameter fields is defined as

$$C_{ijkl}(\mathbf{r})=\sum_g \eta_g^2(\mathbf{r}) a_{ip}^g a_{jq}^g a_{kr}^g a_{ls}^g C_{pqrs}, \tag{2.1}$$

where a_{ij}^g is the transformation matrix representing the rotation of the coordinate system defined on a given grain 'g' with respect to the fixed reference frame and C_{pqrs} is the stiffness tensor of the reference medium. The transformation matrix a_{ij} is expressed in

terms of the Euler angles θ, ψ and ζ (in three dimensions):

$$a_{ij}=\begin{pmatrix}\cos\theta\cos\zeta-\sin\theta\sin\zeta\cos\psi & \sin\theta\cos\zeta+\cos\theta\sin\zeta\cos\psi & \sin\zeta\sin\psi\\ -\cos\theta\sin\zeta-\sin\theta\cos\zeta\cos\psi & -\sin\theta\sin\zeta+\cos\theta\cos\zeta\cos\psi & \cos\zeta\sin\psi\\ \sin\theta\sin\psi & -\cos\theta\sin\psi & \cos\psi\end{pmatrix}, \tag{2.2}$$

where $0\leq\theta\leq 2\pi, 0\leq\psi\leq\pi, 0\leq\zeta\leq 2\pi$. In addition, the elastic constants may depend on additional variables such as concentration and order parameters. However, in this work, we focus on the effect of elastic inhomogeneity in a grain structure.

The spatially dependent elastic stiffness tensor, $C_{ijkl}(\mathbf{r})$, can be written as a sum of a constant homogeneous part C^0_{ijkl} and a position-dependent inhomogeneous perturbation $C'_{ijkl}(\mathbf{r})$. When the homogeneous part is assumed to be isotropic, the homogeneous elastic constants can be expressed in terms of two independent elastic constants, bulk modulus K and shear modulus μ:

$$C^0_{ijkl}=C^{iso}_{ijkl}=K\delta_{ij}\delta_{kl}+\mu\left(\delta_{ik}\delta_{jl}+\delta_{il}\delta_{jk}-\frac{2}{d}\delta_{ij}\delta_{kl}\right), \tag{2.3}$$

where d represents the dimensionality of the system and δ_{ij} is Kronecker's delta function. Otherwise, the homogeneous part can also be approximated as the mean between the maximum and minimum values of $C_{ijkl}(\mathbf{r})$:

$$C^0_{ijkl}=\frac{1}{2}\left[\max(C_{ijkl}(\mathbf{r}))+\min(C_{ijkl}(\mathbf{r}))\right]. \tag{2.4}$$

The remaining elastic constants are treated as inhomogeneous perturbation. Thus $C_{ijkl}(\mathbf{r})$ can be rewritten as

$$C_{ijkl}(\mathbf{r})=C^0_{ijkl}+\left(\sum_g \eta^2_g(\mathbf{r})a^g_{ip}a^g_{jq}a^g_{kr}a^g_{ls}C_{pqrs}-C^0_{ijkl}\right), \tag{2.5}$$

where $g=1,\cdots,Q$ and a^g_{ij} represents the transformation matrix for grain 'g' defined with respect to a fixed coordinate system.

The position-dependent eigenstrain tensor $\epsilon^0_{ij}(\mathbf{r})$ for the entire polycrystal can be specified arbitrarily (dilatational or non-dilatational) and is given by $\epsilon^0_{ij}(\mathbf{r})=\sum_g \eta^2_g(\mathbf{r})a^g_{ip}a^g_{jq}\epsilon^{0,g}_{pq}$, where $\epsilon^{0,g}_{pq}$ is the eigenstrain associated with grain 'g'.

Let $\epsilon_{ij}(\mathbf{r})$ denote the total strain measured with respect to a reference undeformed lattice. Then, assuming linear elasticity, the local stress $\sigma_{ij}(\mathbf{r})$ is given as

$$\sigma_{ij}(\mathbf{r})=(C^0_{ijkl}+C'_{ijkl}(\mathbf{r}))(\epsilon_{kl}(\mathbf{r})-\epsilon^0_{kl}(\mathbf{r})). \tag{2.6}$$

To obtain the local elastic field, we solve the mechanical equilibrium equation

$$\frac{\partial\sigma_{ij}}{\partial r_j}=0 \quad\Rightarrow\quad \nabla_j C_{ijkl}(\mathbf{r})\left(\epsilon_{kl}(\mathbf{r})-\epsilon^0_{kl}(\mathbf{r})\right)=0. \tag{2.7}$$

The total strain $\epsilon_{kl}(\mathbf{r})$ can be expressed as a sum of homogeneous and heterogeneous strains [12]:

$$\epsilon_{ij}(\mathbf{r}) = \bar{\epsilon}_{ij} + \delta\epsilon_{ij}(\mathbf{r}), \tag{2.8}$$

where the homogeneous strain $\bar{\epsilon}_{ij}$ is defined such as

$$\int \delta\epsilon_{ij}(\mathbf{r}) d^3\mathbf{r} = 0. \tag{2.9}$$

The heterogeneous strain field $\delta\epsilon_{ij}(\mathbf{r})$is defined as

$$\delta\epsilon_{ij}(\mathbf{r}) = \frac{1}{2}\left(\frac{\partial u_i(\mathbf{r})}{\partial r_j} + \frac{\partial u_j(\mathbf{r})}{\partial r_i}\right), \tag{2.10}$$

where $u_i(\mathbf{r})$ denotes the ith component of the displacement field.

Using Eqs. (2.5), (2.8) and (2.10) in Eq. (2.7), we obtain after rearranging and simplifying

$$\begin{aligned} C^0_{ijkl}\frac{\partial^2 u_k}{\partial r_j \partial r_l} = &\nabla_j\left[\left(\sum_g \eta_g^2(\mathbf{r}) a^g_{ip} a^g_{jq} a^g_{kr} a^g_{ls} C_{pqrs}\right)\left(\epsilon^0_{kl}(\mathbf{r}) - \bar{\epsilon}_{kl}\right)\right] \\ &- \frac{\partial}{\partial r_j}\left[\left(\sum_g \eta_g^2(\mathbf{r}) a^g_{ip} a^g_{jq} a^g_{kr} a^g_{ls} C_{pqrs} - C^0_{ijkl}\right)\frac{\partial u_k}{\partial r_l}\right]. \end{aligned} \tag{2.11}$$

Following Hu and Chen [6], we implement an iterative perturbation scheme to solve Eq. (2.11) as follows:

Zeroth-order approximation: We assume the elastic moduli to be homogeneous and solve the mechanical equilibrium equation. In other words, $C'_{ijkl}(\mathbf{r})$ is set to zero in Eq. (2.11). Thus we obtain

$$C^0_{ijkl}\frac{\partial^2 u_k(\mathbf{r})}{\partial r_j \partial r_l} = C^0_{ijkl}\nabla_j\left(\epsilon^0_{kl}(\mathbf{r})\right). \tag{2.12}$$

The zeroth-order displacement field is obtained by solving Eq. (2.12) in Fourier space:

$$\tilde{u}^0_k(\mathbf{k}) = -IG_{ik}(\mathbf{n}) k_j \tilde{\sigma}^0_{ij}(\mathbf{k}), \tag{2.13}$$

where $I = \sqrt{-1}$, $\tilde{u}^0_k(\mathbf{k})$ and $\tilde{\sigma}^0_{ij}(\mathbf{k})$ are Fourier transforms of $u^0_k(\mathbf{r})$ and $\sigma^0_{ij}(\mathbf{r})$, respectively, $\mathbf{k}$ is the reciprocal lattice vector, k_j $(j = 1,2,3)$ denotes the jth component of $\mathbf{k}$, $G_{ik}(\mathbf{n})$ is the Green tensor whose inverse is defined as $G^{-1}_{ik}(\mathbf{n}) = C^0_{ijkl} n_j n_l$, $\mathbf{n} = \mathbf{k}/|\mathbf{k}|$, and $\sigma^0_{ij}(\mathbf{r}) = C^0_{ijkl}\epsilon^0_{kl}(\mathbf{r})$.

Higher-order approximation: The higher order solutions for $u_k(\mathbf{r})$ are derived by substituting the zeroth-order displacement solution in the nonlinear term in Eq. (2.11). The nth

order solution $u_k^n(\mathbf{r})$ is obtained using Fourier transforms.

$$\tilde{u}_k^n(\mathbf{k}) = -IG_{ik}(\mathbf{n})k_j \begin{bmatrix} \left(\sum_g \eta_g^2(\mathbf{r}) a_{ip}^g a_{jq}^g a_{kr}^g a_{ls}^g C_{pqrs}\right)\left(\epsilon_{kl}^0(\mathbf{r}) - \bar{\epsilon}_{kl}\right) \\ -\left(\sum_g \eta_g^2(\mathbf{r}) a_{ip}^g a_{jq}^g a_{kr}^g a_{ls}^g C_{pqrs} - C_{ijkl}^0\right) \frac{\partial u_k^{n-1}(\mathbf{r})}{\partial r_l} \end{bmatrix}_{\mathbf{k}}. \tag{2.14}$$

The number of iterations required to refine the displacement solution depends on the accuracy required by the problem. Generally, except for cases with extremely large elastic inhomogeneity, fewer than three iterations are required to achieve convergence of the displacement solution.

When a system is under a constant strain, the homogeneous strain $\bar{\epsilon}_{ij}$ is equal to the applied strain. However, when the boundaries of the system are allowed to relax, the homogeneous strain is obtained by minimizing the total elastic energy. We derive a general expression for homogeneous strain assuming that a constant stress is applied to the system. When the system is subjected to an applied stress σ_{ij}^a, the total elastic energy of the system is given by [13]:

$$F_{el} = \frac{1}{2}\int_V C_{ijkl}(\mathbf{r})[\bar{\epsilon}_{ij} + \delta\epsilon_{ij}(\mathbf{r}) - \epsilon_{ij}^0(\mathbf{r})][\bar{\epsilon}_{kl} + \delta\epsilon_{kl}(\mathbf{r}) - \epsilon_{kl}^0(\mathbf{r})]dV. \tag{2.15}$$

Minimization of total elastic energy with respect to homogeneous strain yields

$$\begin{aligned} & \frac{\partial F_{el}}{\partial \bar{\epsilon}_{ij}} = 0 \\ \Rightarrow \quad & \sigma_{ij}^a = \bar{\epsilon}_{kl}\frac{1}{V}\int_V C_{ijkl}(\mathbf{r})dV + \frac{1}{V}\int_V C_{ijkl}(\mathbf{r})\delta\epsilon_{kl}(\mathbf{r})dV - \frac{1}{V}\int_V C_{ijkl}(\mathbf{r})\epsilon_{kl}^0(\mathbf{r})dV \\ \Rightarrow \quad & \bar{\epsilon}_{kl} = \langle S_{ijkl}\rangle\left(\sigma_{ij}^a + \langle\sigma_{ij}^0\rangle - \langle\delta\sigma_{ij}\rangle\right), \end{aligned} \tag{2.16}$$

where $\langle S_{ijkl}\rangle = \langle C_{ijkl}\rangle^{-1}$, $\langle C_{ijkl}\rangle = (1/V)\int_V C_{ijkl}(\mathbf{r})dV$, $\langle\sigma_{ij}^0\rangle = \frac{1}{V}\int_V C_{ijkl}(\mathbf{r})\epsilon_{kl}^0(\mathbf{r})dV$, and $\langle\delta\sigma_{ij}\rangle = \frac{1}{V}\int_V C_{ijkl}(\mathbf{r})\delta\epsilon_{kl}(\mathbf{r})dV$. Thus, our model can be applied to solve mechanical equilibrium equation in constrained as well as unconstrained systems.

All the parameters in our computation of residual stress distribution have been non-dimensionalized using characteristic length and energy units. In what follows, we present the values of all the parameters in their dimensionless form.

Using our model we have computed the residual stress distribution in polycrystalline systems in two and three dimensions, arbitrarily shaped cavities and cracks with zero elastic modulus, multilayers and composites. The effective elastic constants are calculated using the following assumptions:

i. the elastic modulus changes sharply across the grain boundaries (i.e. no modulus difference between the grain boundaries and the interior);
ii. the excess volume associated with the grain boundaries is negligible (i.e. no volume difference between the grain boundaries and the interior).

It should be noted that assumptions (i) and (ii) are valid when the volume fraction of the grain boundaries in the polycrystal is small. Stress distribution in a polycrystal depends strongly on the variation of elastic constants across the grain boundary. Large stress concentrations at the grain boundaries should affect the overall elastic properties of the polycrystal. Moreover, grain boundaries can be associated with excess volume compared to the grain interior which may lead to relaxation of stress across the grain boundaries. When the volume fraction of the grain boundaries is small i.e. the average grain size is large (of the order of microns) we use a sharp interface assumption to describe the variation of elastic moduli across the grain boundary.

On the other hand, when the volume fraction of the grain boundaries is high (i.e. average grain size of the order of nanometers), assumption (i) is relaxed and the effect of grain boundaries on the calculation of effective elastic properties is taken into account. In this case we assume that the elastic moduli vary smoothly across the grain boundary. As a result, the calculation of effective elastic properties is sensitive to the width of the grain boundary. Further, the grain boundaries are assumed to be elastically softer regions than the grain interior in our calculation. However, in both cases we neglect the volume difference between the grain boundaries and the grain interior in absence of any experimental data regarding the excess volume associated with the grain boundaries.

We have used L^2 norm to measure the error during the refinement procedure. The error, based on the L^2 norm, is defined as follows:

$$error = \sum_{\mathbf{r}} \sqrt{(u_x^{n+1}(\mathbf{r}) - u_x^n(\mathbf{r}))^2 + (u_y^{n+1}(\mathbf{r}) - u_y^n(\mathbf{r}))^2 + (u_z^{n+1}(\mathbf{r}) - u_z^n(\mathbf{r}))^2}, \tag{2.17}$$

where $u_x^{n+1}(\mathbf{r})$, $u_y^{n+1}(\mathbf{r})$ and $u_z^{n+1}(\mathbf{r})$ are the components of displacement obtained after (n+1)th iteration and $u_x^n(\mathbf{r})$, $u_y^n(\mathbf{r})$ and $u_z^n(\mathbf{r})$ are the components of displacement obtained after nth iteration. The iterations are stopped when the error falls below a specified tolerance value. This is used as the convergence criterion for the refinement of displacement solutions.

The tolerance value is set to be 10^{-6} for refinement of displacements; decreasing the tolerance to a smaller value does not affect the accuracy of the solutions. For a system containing cylindrical cavity, the number of iterations required for convergence of the solutions is found to be approximately seven. However, the number of iterations required for convergence of solution increases with the increase in the size of the cavity.

3 Results and discussion

First we consider the example of a cylindrical cavity contained in a uniaxially stressed elastically isotropic solid and compare our numerical solution with the analytical results to prove the accuracy of our method. The system containing cavity is subjected to a uniform tensile stress $\sigma_{xx}^a = 0.01$ along the x-axis. We assumed plane strain condition to compute the residual stress distribution. The system size is chosen to be 1024x1024 grid

points with grid spacing $\Delta x=\Delta y=1.0$. The diameter of the cylindrical cavity is 80 length units. The elastic constants of the solid are assumed to be $C_{11}=450.0$ and$C_{12}=150.0$ and the cavity has zero elastic modulus. The computed residual stress fields inside and around the cavity, $(\sigma_{xx}-\sigma^a_{xx})/\sigma^a_{xx}$, $\sigma_{xy}/\sigma^a_{xx}$ and $\sigma_{yy}/\sigma^a_{xx}$ are shown in Fig. 1(a)-(c). The maximum variation in the stress field is observed around the interface. The numerically computed stress fields along mutually perpendicular x-x and y-y sections through the center of the cavity are in very good agreement with the corresponding analytical solutions available from literature [14] (Fig. 1(d), (e)). Since the system has a cylindrical symmetry, it suffices to show the solutions for one quadrant.

Next, we outline a procedure to calculate effective elastic constants of arbitrary elastically inhomogeneous microstructures. When a material containing inhomogeneities (such as grain boundaries, voids, precipitates) is subjected to an applied strain field, the effective stress field in the material is measured using Eq. (2.6). For a given homogeneous strain and an eigenstrain distribution, the stress field is given by

$$\sigma^{el}_{ij}(\mathbf{r})=C_{ijkl}(\mathbf{r})\left(\delta\epsilon_{ij}(\mathbf{r})+\bar{\epsilon}_{ij}-\epsilon^0_{ij}(\mathbf{r})\right). \tag{3.1}$$

The average stress in the material σ^{av}_{ij} is calculated as

$$\sigma^{av}_{ij}=\frac{1}{V}\int_V\sigma_{ij}(\mathbf{r})dV. \tag{3.2}$$

The effective elastic stiffness tensor C^{eff}_{ij} (in Voigt notation) is obtained by measuring the overall stress response when the system is subjected to applied strain (constrained system):

$$\sigma^{av}_i=C^{eff}_{ij}\bar{\epsilon}_j. \tag{3.3}$$

To ensure the correctness of our method and to test the sharp interface assumption for the variation of elastic moduli across the interface, we calculated the effective elastic moduli of a three-dimensional multilayered composite using our method and compared them with the analytically obtained elastic moduli [15]. The multilayered composite, shown in Fig. 2, is composed of alternating elastically isotropic layers stacked perpendicular to the x-axis. The elastic moduli of the materials constituting the red and blue layers are isotropic but they vary in magnitude ($C_{11}=450$, $C_{12}=150$ for the red layer and $C_{11}=225$, $C_{12}=75$ for the blue layer). The solutions converged after the first iteration and we obtained an excellent match between the computed effective elastic constants of this transversely isotropic composite and the corresponding analytical values (see Table 1).

We also calculated the effective elastic constants of two- and three-dimensional polycrystals. Fig. 3(a) shows a two-dimensional single phase polycrystalline microstructure containing randomly oriented and elastically anisotropic grains (having cubic symmetry). The elastic constants of the phase are $C_{11}=450.0$, $C_{12}=150.0$ and $C_{44}=300.0$. The normalized components of the residual stress field, $\sigma_{xx}/\sigma^a_{xx}$, $\sigma_{xy}/\sigma^a_{xx}$, $\sigma_{yy}/\sigma^a_{xx}$, are shown in Fig. 3(b)-(d) when the polycrystal is subjected to a uniaxial applied stress $\sigma^a_{xx}=0.01$.

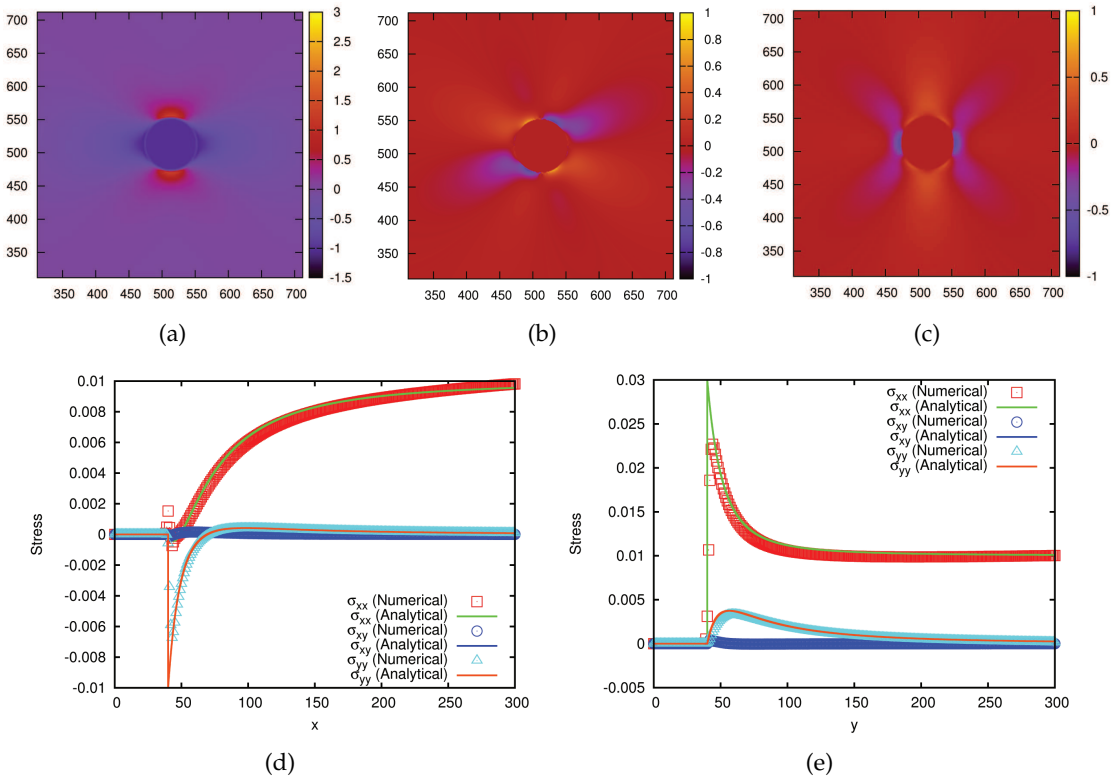

Figure 1: Equilibrium residual stress fields (a) $(\sigma_{xx}-\sigma^a_{xx})/\sigma^a_{xx}$, (b) $\sigma_{xy}/\sigma^a_{xx}$, (c) $\sigma_{yy}/\sigma^a_{xx}$ in a uniaxially stressed elastically isotropic solid containing a cylindrical cavity. Stress is applied along x-axis ($\sigma^a_{xx}=0.01$). The box dimensions in figures (a)-(c) correspond to 400x400 length units. (d),(e) Comparison of numerically obtained stress fields with the corresponding analytical solutions along x-x and y-y sections passing through the center of the cavity parallel to x- and y-axis, respectively. Numerical solutions are represented by open symbols and the analytical solutions are represented by lines.

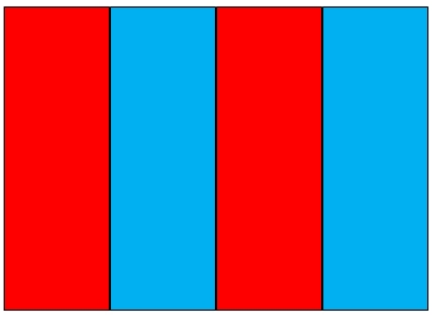

Figure 2: A multilayered composite containing alternating layers. Both red and blue layers have isotropic elastic constants. The elastic constants of the material comprising the red layers are $C_{11}=450, C_{12}=150$ and that of the material comprising the blue layers are$C_{11}=225, C_{12}=75$.

Table 1: Comparison between computationally obtained values of effective elastic constants using our model and the corresponding analytical values in a multilayered composite material.

Effective Elastic Constants	Analytical	Simulation
C_{11}^{eff}	300.0	300.0
$C_{12}^{eff}=C_{13}^{eff}$	100.0	100.0
$C_{22}^{eff}=C_{33}^{eff}$	333.33	333.3333
C_{23}^{eff}	108.33	108.3333
C_{44}^{eff}	112.5	112.5
$C_{55}^{eff}=C_{66}^{eff}$	100.0	100.0

The stress field is inhomogeneous due to the variation of elastic moduli with grain orientation. The stress field near the grain boundaries is different from that of the grain interior. The grain boundaries are associated with different levels of stress concentration depending on the misorientation between the grains. For example, the grain boundaries that are favorably aligned with respect to the direction of applied stress are associated with lower stress concentration.

We have also evaluated the effective elastic properties of the polycrystal from the mechanical response assuming no modulus and volume differences between the grains and the grain boundaries. In the calculation of effective elastic constants, the volume fraction of grain boundaries is assumed to be small compared to the grain interior and sharp interface assumption is used to describe the variation of elastic moduli across the grain boundaries.

The computed effective elastic constants are $C_{11}^{eff}=C_{22}^{eff}=502.145$, $C_{12}^{eff}=97.855$, $C_{44}^{eff}=212.057$ which indicates elastically isotropic properties even though the grains have cubic anisotropy. The Voigt averaged elastic constants are $C_{11}^{Voigt}=520.1573$, $C_{12}^{Voigt}=79.801$, and $C_{44}^{Voigt}=229.816$ [16]. The computed elastic constants are close to the Voigt averaged values which provide the upper bound of the effective elastic moduli of the polycrystal.

We also computed the effective elastic properties of a three-dimensional polycrystalline microstructure (Fig. 4(a)) generated using phase field method. The microstructure is described using 100 order parameters and the computational domain size is $64\times64\times64$. The grains are assumed to be randomly oriented and the crystal has cubic elastic anisotropy and the same elastic constants as the previous example. The local pressure distribution, when the system is subjected to an applied stress $\sigma_{xx}^{a}=0.01$ is shown in Fig. 4(b).

The computed values of the effective elastic constants using sharp interface assumption for the variation of elastic moduli across the grain boundaries lie close to the macroscopic Voigt averaged values (see Table 2). However, if we relax the sharp interface assumption and take into account the effect of grain boundaries, the calculated effective elastic moduli are smaller in magnitude. This result stems from our definition of position dependent elastic stiffness tensor in Eq. (2.1). The values of the calculated elastic

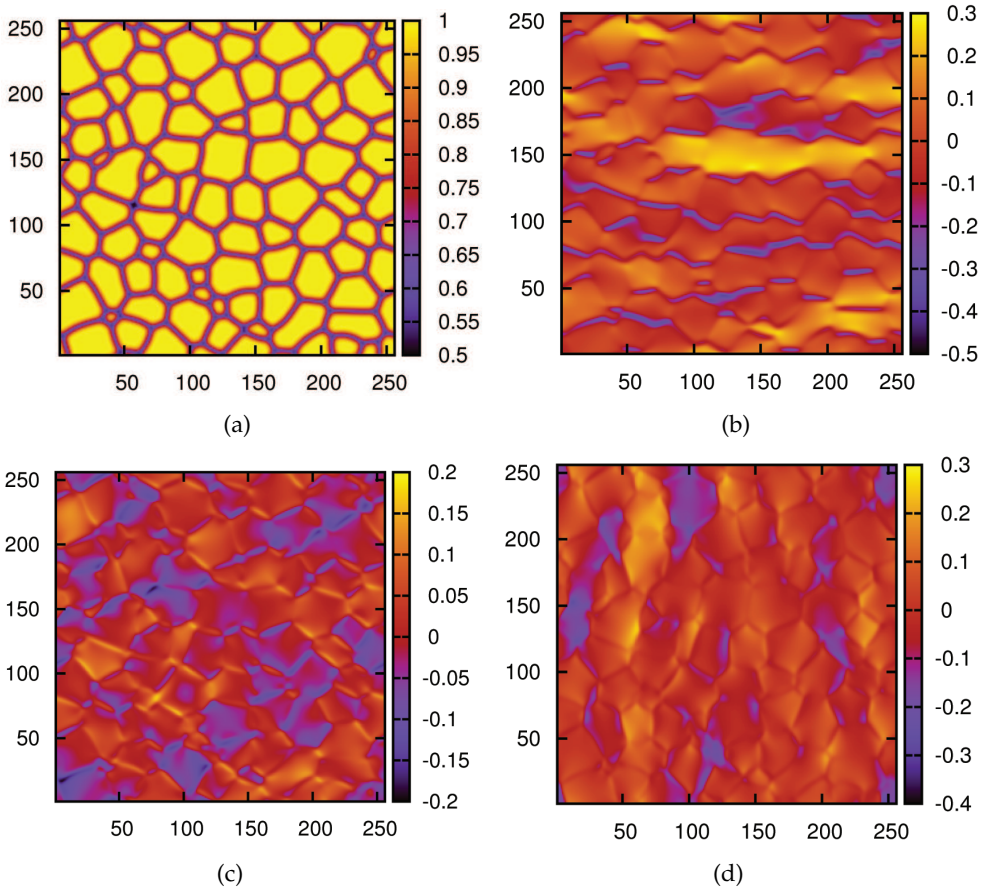

Figure 3: (a) A randomly textured polycrystal (in two dimensions) containing elastically anisotropic grains having cubic symmetry. The polycrystal is subjected to uniform tensile stress along x-axis. (b)-(d) Equilibrium stress fields σ_{xx}, σ_{xy} and σ_{yy}, respectively, scaled with respect to the applied stress.

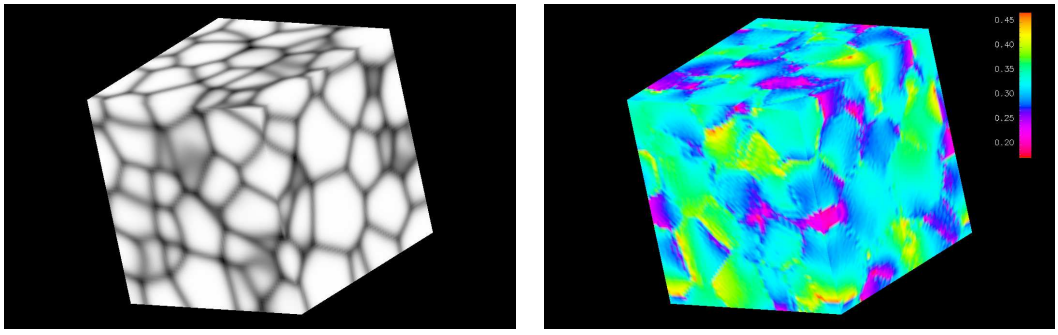

Figure 4: (a) A three dimensional polycrystal containing randomly oriented elastically anisotropic grains with cubic symmetry. The polycrystal is subjected to an uniaxial stress along x direction ($\sigma_{xx}=0.01$). (b) Local pressure distribution $p(\mathbf{r})$ $(=(\sigma_{xx}+\sigma_{yy}+\sigma_{zz})/3.0)$ in the polycrystal scaled with respect to applied stress.

Table 2: Comparison of effective elastic constants obtained from iterative perturbation technique using sharp and diffuse interface assumptions for the variation of elastic moduli across the grain boundary, respectively, and those estimated using Voigt approximation for a 3D polycrystal.

Effective elastic constants	Computed from phase field model (sharp interface assumption)	Computed from phase field model (diffuse interface assumption)	Estimated using Voigt approximation
C_{11}^{eff}	534.713	395.751	552.1
C_{22}^{eff}	537.13	414.104	554.0969
C_{33}^{eff}	517.276	343.42	535.0264
C_{12}^{eff}	97.71	15.45	89.47
C_{13}^{eff}	117.57	93.2	108.63
C_{23}^{eff}	115.155	89.8	106.71
C_{44}^{eff}	245.96	187.86	256.69
C_{55}^{eff}	248.578	168.678	258.645
C_{66}^{eff}	226.98	128.98	239.48

constants using sharp and diffuse interface descriptions for the change in moduli across grain boundaries are compared in Table 2. The moduli calculated using diffuse interface assumption are also sensitive to the width of the grain boundary.

It should be noted that the number of iterations required for convergence increase from 3 to 5, when the number of order parameters is increased ten times. Since our model only keeps track of the nonzero active order parameters for computing the residual stress fields in polycrystals, there is no significant increase in the number of iterations for a corresponding increase in the number of order parameters [17].

The model developed by Wang et al. requires the evaluation of equivalent eigenstrain which is obtained as a steady state solution of the time-dependent Ginzburg-Landau equation [8]. On the other hand, our model is based on an iterative perturbation method. Both of these methods can be implemented in three dimensions and can tackle problems involving arbitrary distribution of elastic constants and eigenstrain. Since the computational time required is not explicitly mentioned by Wang et al., it is difficult to compare the relative efficiency of the methods. However, our method does not require steady state solution of Ginzburg-Landau equation. The accuracy of our method depends on the number of higher-order refinements of the displacement solution (even in systems with extremely large difference in elastic modulus such as voids and cavities the number of higher-order corrections is approximately seven). Moreover, the equilibrium stress distribution obtained for cavities and polycrystals using our method agree well with those obtained by Wang et al.

In a recent study Ni and Chiang used phase field microelasticity model based on the concept of equivalent eigenstrain to predict the elastic constants of three-dimensional heterogeneous materials [18]. Their results show that for an infinite isotropic elastic medium

containing a spherical void under uniaxial loading, the number of iterative time steps required for attaining convergence with a relative error less than 1% is approximately six when the stiffness contrast (i.e. the ratio of shear modulus between phases) is 1e-3. When the relative error is smaller, the number of time steps required for convergence increase to a larger value. However, when our iterative method is applied to such a system under similar conditions for convergence, the number of iterations required is two.

In summary, we have developed a phase field method to calculate residual stress distribution in arbitrary structurally and elastically inhomogeneous materials. Our method can be applied to materials with very large modulus contrast. Moreover, our model can be employed to calculate the effective properties of polycrystals with a high accuracy.

Acknowledgments

The authors would like to acknowledge the financial supports from the National Science Foundation under the grant number DMR-0710483.

References

[1] M. Doi, Elasticity effects on the microstructure of alloys containing coherent precipitates, Prog. Mater. Sci., 40 (1996), 79.
[2] P. Fratzl, O. Penrose and J. Lebowitz, Modeling of phase separation in alloys with coherent elastic misfit, J. Stat. Phys., 95 (1999), 1429.
[3] L.-Q. Chen, Phase-field models for microstructural evolution, Ann. Rev. Mater. Res., 32 (2002), 113.
[4] P. H. Leo, J. S. Lowengrub and H. J. Jou, A diffuse interface model for microstructural evolution in elastically stressed solids, Acta Mater., 46 (1998), 2113.
[5] J. Zhu, L.-Q. Chen and J. Shen, Morphological evolution during phase separation and coarsening with strong inhomogeneous elasticity, Modell. Simul. Mater. Sci. Eng., 9 (2001), 499.
[6] S. Y. Hu and L.-Q. Chen, A phase-field model for evolving microstructures with strong elastic inhomogeneity, Acta Mater., 49 (2001), 1879.
[7] P. Yu, S. Y. Hu, L.-Q. Chen and Q. Du, An iterative-perturbation scheme for treating inhomogeneous elasticity in phase-field models, J. Comput. Phys., 208 (2005), 34.
[8] Y. U. Wang, Y. M. Jin and A. G. Khachaturyan, Phase field microelasticity theory and modeling of elastically and structurally inhomogeneous solid, J. Appl. Phys., 92 (2002), 1351.
[9] Y. M. Jin, Y. U. Wang and A. G. Khachaturyan, Three-dimensional phase field microelasticity theory and modeling of multiple cracks and voids, Appl. Phys. Lett., 79 (2001), 3071.
[10] D. Fan and L.-Q. Chen, Computer simulation of grain growth using a continuum field model, Acta Mater., 45 (1997), 611.
[11] D. Fan, C. Geng and L.-Q. Chen, Computer simulation of topological evolution in 2-D grain growth using a continuum diffuse-interface field model, Acta Mater., 45 (1997), 1115.
[12] A. G. Khachaturyan, Theory of Structural Phase Transformations in Solids, John Wiley and Sons, New York, 1983.
[13] D. Y. Li and L.-Q. Chen, Shape evolution and splitting of coherent particles under applied stresses, Acta Mater., 47 (1998), 247.

[14] T. Mura, Micromechanics of Defects in Solids, Springer, 1987.
[15] S. Torquato, Random Heterogeneous Materials: Microstructure and Macroscopic Properties, Springer, 2002.
[16] J. M. J. den Toonder, J. A. W. van Dommelen and F. P. T. Baaijens, The relation between single crystal elasticity and the effective elastic behaviour of polycrystalline materials: Theory, measurement and computation, Modell. Simul. Mater. Sci. Eng., 7 (1999), 909.
[17] S. Vedantam and B. S. V. Patnaik, Efficient numerical algorithm for multiphase field simulations, Phys. Rev. E, 73 (2006), 016703.
[18] Y. Ni and M. Chiang, Prediction of elastic properties of heterogeneous materials with complex microstructures, J. Mech. Phys. Solids, 55 (2007), 517.